IJCRT.ORG ISSN : 2320-2882

INTERNATIONAL JOURNAL OF CREATIVE RESEARCH THOUGHTS (IJCRT)

An International Open Access, Peer-reviewed, Refereed Journal

Microstructural Transformation and Heat Treatment of 11Cr-9Ni Martensitic Stainless Steel

Zafar Imam[1*], B. N. Roy[1], Anil K. Rajak[1], S. Hembrom[1], S. K. Sharma[1]

[1]Department of Metallurgical Engineering BIT SINDRI

ABSTRACT

This study investigates the effects of various annealing treatments on the microstructural evolution and mechanical properties of low carbon-11Cr-9Ni martensitic stainless steel intended for cryogenic applications. Samples were subjected to different heat treatment conditions at 350°C, 550°C, and 600°C, followed by either air cooling or liquid nitrogen quenching. Microstructural characterization was performed using Scanning Electron Microscopy (SEM), while retained austenite content was quantified through X-Ray Diffraction (XRD) analysis using MAUD software and Integrated Intensity Method. The results revealed that samples annealed at 550°C for 2 hours, followed by air cooling and aging at 370°C for 5 hours, exhibited the highest retained austenite content (45.61%). Conversely, samples subjected to identical annealing conditions but quenched in liquid nitrogen showed minimal retained austenite (2.00%) due to austenite instability at cryogenic temperatures. Samples annealed at 350°C demonstrated low retained austenite content (2.87%) attributed to sluggish diffusion of austenite stabilizers. Hardness measurements indicated that liquid nitrogen quenched samples consistently displayed higher hardness values compared to their air-cooled counterparts, with the 350°C annealed and liquid nitrogen quenched sample exhibiting the highest hardness among all heat-treated specimens.

Keywords: Microstructure, Heat Treatment, Martensitic Stainless Steel, Hardness

1. INTRODUCTION

There is a great deal of interest at present in developing high-strength properties in construction steels. At the same time, increased toughness is often required. The troublesome task of fulfilling these combined conditions in a reasonably economic way has emphasized the need for more detailed information about relationship between microstructure, strength, and toughness So, in order to impart the above mentioned properties we need a material having martensitic structure for imparting hardness as

well as some amount of retained austenite to impart ductility. So, in our present study we will be focusing mainly on martensitic grade steel and we will try to retain some austenite in the microstructure. Thus control of microstructure for achieving the desired properties in the steel is required. These steels are preferred for applications which require high strength plus stiffness and corrosion resistance and should be cost effective [1-2]. The major applications include hydraulic turbines ,actuators, pumps, valves, components in offshore structure and petrochemical and power plants and certainly high spaced aerospace components (mainly for making cryogenic fuel container).

The as cast ingot containing different phases like pearlite and ferrite is homogenized to get fully austenitic structure and then quenched to get the martensitic structure and some retained austenite. Austenite that is cooled very rapidly can form martensite. During quenching, the rate of diffusion is lowered to such an extent that no transformation dependent on diffusion can take place during transformation gamma iron changes to alpha iron [3]. As no diffusion of carbon and other metallic atoms can take place at such a low transformation temp, the chemical composition of alpha iron will be same as that of gamma iron. As solubility of carbon is more in gamma iron than in alpha iron, the alpha iron thus form becomes supersaturated. It has body-cantered tetragonal (BCT) structure. This non equilibrium phase can only transform at lower temperature, where the driving force for the reaction is sufficient to overcome the considerable lattice strain imposed by the transformation. This transformation is a thermal in nature. Then this quenched material is again heat treated so that partitioning of alloying elements takes place such that the austenite stabilizers like Nickel diffuses into gamma phase and alpha stabilizers like Mo and Nb diffuses into alpha or BCC phase in order to stabilize them. After that this material undergo different treatments like air cooling after annealing, liquid nitrogen quenching after annealing and so on .After that their properties and microstructure are observe and the respective amount of retained austenite and martensite is measured [4-6].

So, the aim of our present study is to obtain a microstructure which has some stabilized austenite to impart impact and ductility and a major part of martensite in order to impart hardness and tensile strength.

2. LITERATURE REVIEW

With the increasing demand for materials to withstand high corrosive environment and with excellent mechanical properties there is a need to alter the amount of different phases present in the microstructure**.** In order to alter the amount of different phases scientist has given different methods of heat treatment and different alloy additions in order to stabilize different phases according to our need Anoop et. al. [1] has shown that precipitation hardenable steels are a specialized class of stainless steels, which are characterized by high to ultra-high strength levels, excellent toughness, good corrosion resistance and adequate fabricability. These steels have successfully filled the technological gap between tough

and corrosion resistance austenitic steels with lower strength and with martensitic stainless steels with higher strength and lower toughness. The mechanical properties of these steels depend primarily on the nature and distribution of precipitates, the presence of retained austenite and the prior austenite grain size [7]. Fine prior austenite grain size is an essential requirement for obtaining a good combination of impact toughness and ductile-to- brittle transition temperature (DBTT) for martensitic precipitation hardenable steels without any compromise in strength [8]. The experiments done by Anoop et. al. [1] shows that the impact Toughness of 12Cr-10Ni steel in solution treated and solution treatment followed by 250°C aged condition is not significantly affected by solution treatment temperature, when tested at room temperature and 77k. The charpy impact value at 77k was about 93 j and yield strength about 79805MPa. Austenitic stainless steel are the most widely used structural material for cryogenic applications. However low yield strength (~250MPa) is a major drawback for this material [9-10]. According to a research paper some of the martensitic stainless steel containing low carbon can give rise to increased mechanical strength and corrosion resistance by just adding a very small amount of Mo [11-12]. According to the same paper Ni and Ti can also be added as stabilizing elements to form carbides and nitrides. According to Rodigues et al TiC fine carbides promotes the refinement of the microstructure and increases the mechanical properties. Boron addition refined the microstructure and increased the hardness and wear resistance by metal boron precipitate**.** Since Mo can reduce the rate of formation of NbC, high strength low-alloy steels are generally formed by the simultaneous addition of Nb and Mo to reduce the growth rate of carbide and to increase its strength [13-16].

3. EXPERIMENTAL PROCEDURES

3.1 Material and Heat treatment

The chemical composition of experimental steel is presented in Table. 1.

Table.3.1.Chemical composition of the martensitic stainless steel in this study (wt. %).

Elements	Cr	Ni	Mo	Mn	Si	Ti	C	Nb	P	S	Al
wt%	11	9	0.6	0.4	0.335	0.297	0.059	0.043	0.018	0.04	0.02

A 8 kg ingot was made in an air induction melting furnace and then a lollypop sample is taken out in a lollypop kind of mould from the molten metal using vacuum and then sent for the Direct Reading Spectroscopy (DRS) where the exact Composition of the melt was calculated If the composition is not up to the level then further addition of the alloy would be done. Then the molten metal is poured in the preheated mould and is allowed to cool in air.

Furnace Used For Melting the Ingot – The furnace used was a kind of air induction furnace whose coil is made of 99% pure copper induction wire. Mica is used for insulating the induction wire from earth and furnace body and the furnace is lined with

MgO refractory bricks. The furnace casing is made from mild steel.

Power Required For the Operation Of Air Induction Furnace – Around 15 kW power is required for melting the ingot along with the alloy additions and around 1600°C is obtained for melting the ingot.

Deoxidation of the Melt – During melting of the ingot oxygen gets into the melt from the atmosphere and if these were not excluded then it may oxidize other alloy elements and form inclusions in the casting and sound casting will not be achieved. To get a sound casting the molten bath is deoxidized with aluminium. Al is added in the last stage of melting to form aluminium oxide which moves to the top of the melt and forms a part of slag. **Mould and Ladle -** The mould used in melting the ingot is made of cast iron and the ladle is also made from the same material. Ladle is used to carry the molten metal from the furnace to the mould. Ladle is preheated before pouring molten metal into it. In our experiment we have preheated the ladle using coke oven gas bought from TISCO Plant nearby.

Homogenization of the Casting – Homogenization of the casting is necessary before any further operation. During solidification of the cast many problems like segregation, inhomogeneous distribution of the alloying elements takes place. Therefore homogenization absorbs the segregation and coring found in casting and produces a more homogeneous and uniform structure to meet our requirement for the further operations. After cooling the cast it was homogenized in a muffle furnace for 3 hours at 1200°C.

Quenching after Homogenization– Quenching is done in order to obtain a martensitic structured steel. Same is done in our experiment. We quenched the homogenized stainless steel in water. The ingot is hold with tong and is put into the water bath and is continuously stirred to avoid vapor formation around the ingot which hinders the heat transfer from ingot to water.

Sample Cutting - After proper homogenization samples of dimension 2x2 cm were cut from that homogenized ingot. Power saw using circular carbide blade is used for cutting samples to desired size. Each sample is given different heat treatments. The list of heat treatments after homogenization is as follows:

Heat treatment done at 350°C

1. Heat treated at 350°C for two hours and then air cooled.
2. Heat treated at 350°C for two hours and then air cooled and then quenched in liquid nitrogen

Heat treatment done at 550°C1.

1. Heat treated at 550°C and then air cooled.
2. Heat treated at 550°C and then air cooled and then quenched in liquid nitrogen.
3. Heat treated at 550°Cand then air cooled and then aged for 5 hours at 370C

Heat treatment done at 600°C1.

1. Heat treated at 600°C and then air cooled.
2. Heat treated at 600°C and then air cooled and then quenched in liquid nitrogen.
3. Heat treated at 600°C and then air cooled and then aged for 5 hours at 370°C.

All the above heat-treated samples along with one homogenized sample were prepared for microstructure analysis and hardness testing. **3.2 Metallography**

Metallography consist of the following steps:

(i) Sectioning

(ii) Mounting (optional)

(iii)Grinding

(iv)Polishing

(v) Etching.

Sectioning – This is the most important step in preparing specimens for physical or microscopic analysis. Microstructure should not be altered during sectioning and practically hot and cold working accompanies most sectioning methods. There are different sectioning methods which includes fracturing (by using hammer), shearing, sawing (using hacksaw, band saw and wire saws), and electric discharge machining (this process uses sparks in a controlled manner to remove Material from a conducting work piece in a dielectric fluid like kerosene). In our experiment we cut samples using power operated round circular saw.

Mounting – Small or oddly shaped specimens are mounted to facilitate easy handling during preparation and examination. Bakelite and diallyl phthalate are thermosetting resins which are most widely used as molding material. Transparent methyl methacrylate, polystyrene, polyvinyl chloride (PVC) is some of the thermoplastic resins used in molding. Heat and pressure is used during molding. Thermosetting molds can be ejected from the mold at the molding temperature while thermoplastic resins must be cooled to ambient temperature under pressure**.**

Grinding – We prepare the cut surface suitably for metallographic examinations as optically flat, reflective, smooth and scratch free. Samples were rough grinded using 80 grit sizes and then fine grinded using emery papers of grade 220 to 2500 grit sizes. We should start from 80 grit size emery paper and then we increase the emery grit size no. each time changing the emery paper we rotate the sample by 90°.

Polishing - After fine grinding, samples were cloth polished using alumina slurry (alumina powders having different sizes down to 0.05μm) and colloidal solution to get mirror polished surface.

Etching – It is used in metallography primarily to reveal the microstructure of a specimen under the optical microscope. In our experiment polished metallographic samples were etched with Villela's reagent (90ml distilled water, 10ml HCl and 1 gm picric acid) for 15 to 20 seconds in order to reveal the microstructure constituents of the steel. Finally, etched samples were observed under optical microscope and scanning electron microscope (SEM) to analyze the microstructural constituents.

3.3 Optical Microscopy

Optical microscope was used for optical microscopy. It is often referred to as the light microscope that commonly uses visible light and a system of lenses to Magnify images of small objects.

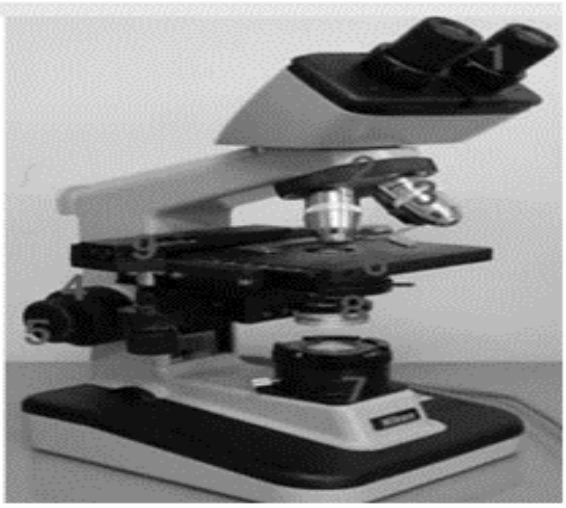

Fig. 3.1- Different parts of optical microscope

The above pictures show an optical microscope whose different parts are labelled with no. 1 to 9.

1. Eyepiece
2. Objective turret, revolver, or revolving nose piece (to hold multiple objective lenses)
3. Objective lenses Focus knobs (to move the stage)
4. Coarse adjustment
5. Fine adjustment
6. Stage (to hold the specimen)
7. Light source (a light or mirror)
8. Diaphragm and condenser
9. Mechanical stage.

In our current experiment LEICA DM-2500M metallurgical microscope was used in the magnification range from 50X-1000X

3.4 Microstructural Evolution of martensitic stainless steel Using SEM

A scanning electron microscope (SEM) is a type of electron microscope that produces images of a sample by scanning the surface with a focused beam of electrons. The electrons interact with atoms in the sample, producing various signals that contain information about the surface topography and composition of the sample. The electron beam is scanned in a raster scan pattern and the position of the beam combined with the intensity of the detected signal to produce an image. In the most common SEM mode, secondary electrons emitted by atoms excited by the electron beam are detected using a secondary electron detector. SEM can achieve resolution better than 1 nanometre.

Principle and capacity of SEM -

The signals used by a scanning electron microscope to produce an image result from interactions of the electron beam with atoms at various depths within the sample. Various types of signals are produced including secondary electrons (SE), reflected or back-scattered electrons (BSE), characteristic X-rays and light (cathodoluminescence) (CL), absorbed current (specimen current) and transmitted electrons. Secondary electron detectors are standard equipment in all SEMs, but it is rare for a single machine to have detectors for all other possible signals. Secondary electrons have very low energies on the order of 50 eV, which limits their mean free path in solid matter. Consequently, SEs can only escape from the top few nanometres of the surface of a sample. The signal from secondary electrons tends to be highly localized at the point of impact of the primary electron beam, making it possible to collect images of the sample surface with a resolution of below 1 nm. Back-scattered electrons (BSE) are beam electrons that are reflected from the sample by elastic scattering. They emerge from deeper locations within the specimen and, consequently, the resolution of BSE images is less than SE images. However, BSE are often used in analytical SEM, along with the spectra made from the characteristic X- rays, because the intensity of the BSE signal is strongly related

to the atomic number (Z) of the specimen. BSE images can provide information about the distribution, but not the identity, of different elements in the sample. In samples predominantly composed of light elements, such as biological specimens, BSE imaging can image colloidal gold immune labels of 5 or 10 nm diameters, which would otherwise be difficult or impossible to detect in secondary electron images. Characteristic X-rays are emitted when the electron beam removes an inner shell Electron from the sample, causing a higher-energy electron to fill the shell and release energy. The energy or wavelength of these characteristic X-rays can be measured by Energy-dispersive X-ray spectroscopy or Wavelength-dispersive X-ray spectroscopy and used to identify and measure the abundance of elements in the sample and map their distribution.

Due to the very narrow electron beam, SEM micrographs have a large depth of field yielding a characteristic three-dimensional appearance useful for understanding the surface structure of a sample. This is exemplified by the micrograph of pollen shown above. A wide range of magnifications is possible, from about 10 times (about equivalent to that of a powerful hand- lens) to more than 500,000 times, about 250 times the magnification limit of the best light microscopes.

Scanning process and image formation in SEM –

In a typical SEM, an electron beam is thermionically emitted from an electron gun fitted with a tungsten filament cathode. Tungsten is normally used in thermionic electron guns because it has the highest melting point and lowest vapor pressure of all metals, thereby allowing it to be electrically heated for electron emission, and because of its low cost. Other types of electron emitters include lanthanum hexaboride (LaB) cathodes, which can be used in a standard tungsten filament SEM if the vacuum system is upgraded or field emission guns (FEG), which may be of the cold-cathode type using tungsten single crystal emitters or the thermally assisted Schottky type, that use emitters of zirconium oxide.

The electron beam, which typically has an energy ranging from 0.2keV to 40keV, is focused by one or two condenser lenses to a spot about 0.4nm to 5nm in diameter. The beam passes through pairs of scanning coils or pairs of deflector plates in the electron column, typically in the final lens, which deflect the beam in the x and y axes so that it scans in a raster fashion over a rectangular area of the simple surface.

Mechanisms of emission of secondary electrons, backscattered electrons, and characteristic X-rays from atoms of the sample:

When the primary electron beam interact with the sample, the electron lose energy by repeated random scattering and absorption with a teardrop shaped volume of the specimen known as the interaction volume, which extends from less than 100nm to approximately 5µm into the surface. The size of the interaction volume depends on the electron's landing energy, the atomic no. of the specimen and the specimen's density. The Energy exchange between the electron

beam and the sample results in the reflection of high energy electrons by elastic scattering, emission of secondary electrons by inelastic scattering and emission of electromagnetic radiation, each of which can be detected by specialized detector. The beam current absorbed by the specimen can also be detected and used to create images of the distribution of specimen current. Electronic amplifier of various types are used to amplify the signals, which are displayed as variation in brightness on a computer monitor each pixel of computer video memory is synchronized with the position of the beam on the specimen in the microscope and the resulting image is therefore a distribution map of the intensity of the signal being emitted from the scanned area of the specimen.

In our experiment the microstructures of annealed samples were characterized by a Nova Nano SEM 430, FEI Company. The samples were ultrasonically cleaned and polished mechanically then etched by Villela's reagent whose composition was 90 ml distilled water, 10 ml HCl and 1 gm picric acid (trinitrophenol). After etching the samples were put in SEM and their microstructure was analyzed.

3.4 XRD analysis of martensitic stainless steel

X-ray scattering techniques are a family of non-destructive analytical techniques which reveal information about the crystal structure, chemical composition, and physical properties of materials and thin films. These techniques are based on observing the scattered intensity of an X-ray beam hitting a sample as a function of incident and scattered angle, polarization, and wavelength or energy.

An introduction to X-ray diffraction - The scattered X-rays from the sample interfere with each other either constructively or destructively. This means that detectors can read-out a signal only at angles where constructive interference occurs. This is schematically shown in the next picture.

The dots in the graph correspond to the building blocks of a crystalline material. Due to the crystalline nature, the atoms are arranged periodically. The incident X-ray beam is scattered at different planes of the material. The resulting diffracted X-rays therefore have a different optical path length to travel. The magnitude of this path length only depends on the distance between the Crystal planes and the incident angle of the X-ray beam.

This is summarized in the famous Bragg – Equation:

$$n\lambda=2d\sin\theta \qquad (1)$$

This equation can be described as follows: constructive interference occurs only if the path difference (given by 2d sinθ) is a multiple (n=1,2,..) of the used wavelength of the X-ray beam. As the wavelength in XRD experiments is known and the angles at which constructive interference occurs are measured, the use of the Bragg equation allows determining the distance between the lattice planes of the material.

The result of the measurement is a so called diffractogramm. This is a plot of X-ray intensity on the y-axis versus the angle 2θ (2θ is defined as the angle between the incident and the diffracted beam) on the x-axis.

The volume fraction of retained austenite was

measured by a Bruker 8 Discover X-ray diffractometer (operated at 40 kV, 182 mA) with Cu Kα radiation at room temperature. During the experiment, a 2θ range from 40° to 105° was step-scanned with a scanning speed of

1.5second per step with step size of 0.02. The specimens for X-ray diffraction (XRD) measurements were mechanically ground and finally electro-polished to minimize the possible error originating from the mechanically induced transformation of retained austenite during the sample preparation. Integrated intensities of the (200)α and (211)α peaks as well as (200)γ, (220)γ and (311)γ peaks were used to estimate the austenite content. The volume fraction of the austenite was calculated using MAUD software and by Integrated intensity method using ORIGIN software. The volume fraction of the austenite Vγ was calculated using the equation **Vγ = 1,4Iγ / (Iα + 1.4Iγ (2)**

Where γ I is the integrated intensity of austenite and Iα is the integrated intensity of ferrite.

4. Results and Discussion

4.1. Optical image of as cast sample

Dendritic structure of the as cast structure near mould surface small amount of equiaxed grain at the centre.

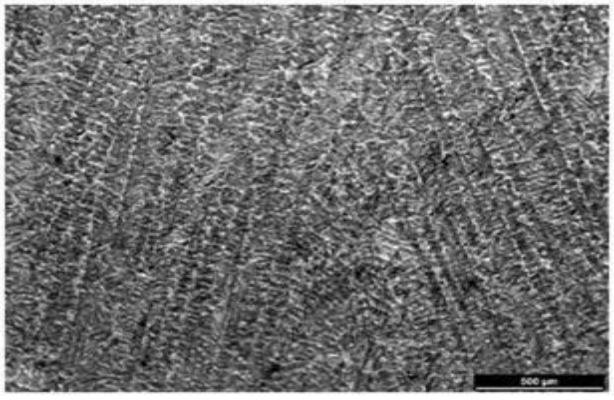

(a)

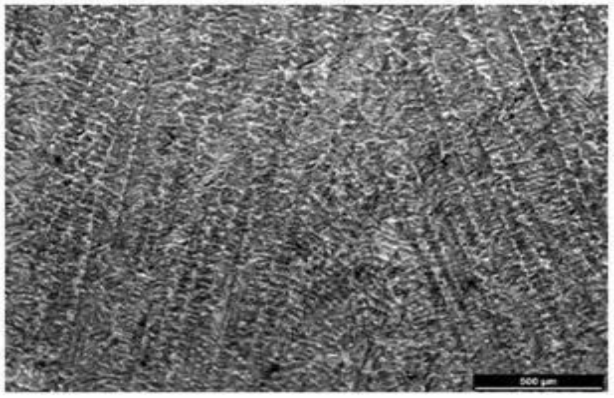

(b)

Figure 4.1-(a) long dendritic structure in the as cast material near at the surface of the mould and (b) equiaxed structure near at the middle of the as cast sample.

4.2. SEM images of annealed samples

4.2.1. Sample heated at 350°C for two hours and then air cooled

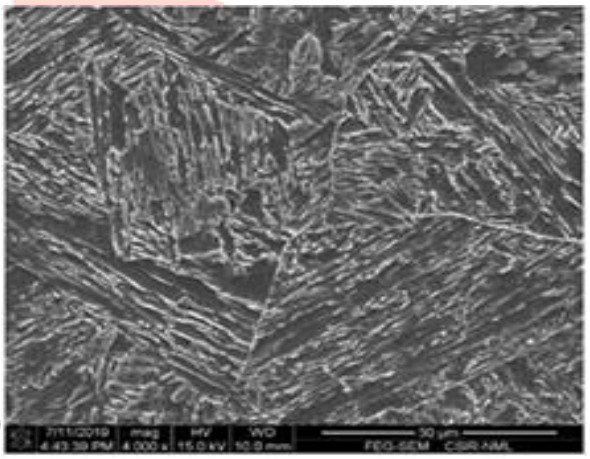

(a)

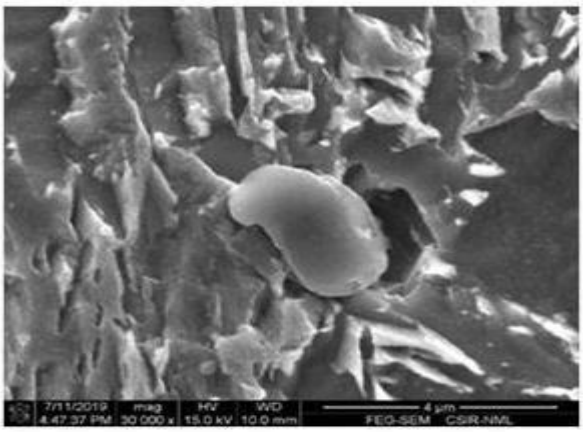

(b)

Figure 4.2-(a) lath like structure of martensite and (b) represents the inclusion MnS and this is

confirmed by EDAX analysis and the EDAX data for this sample is shown above:

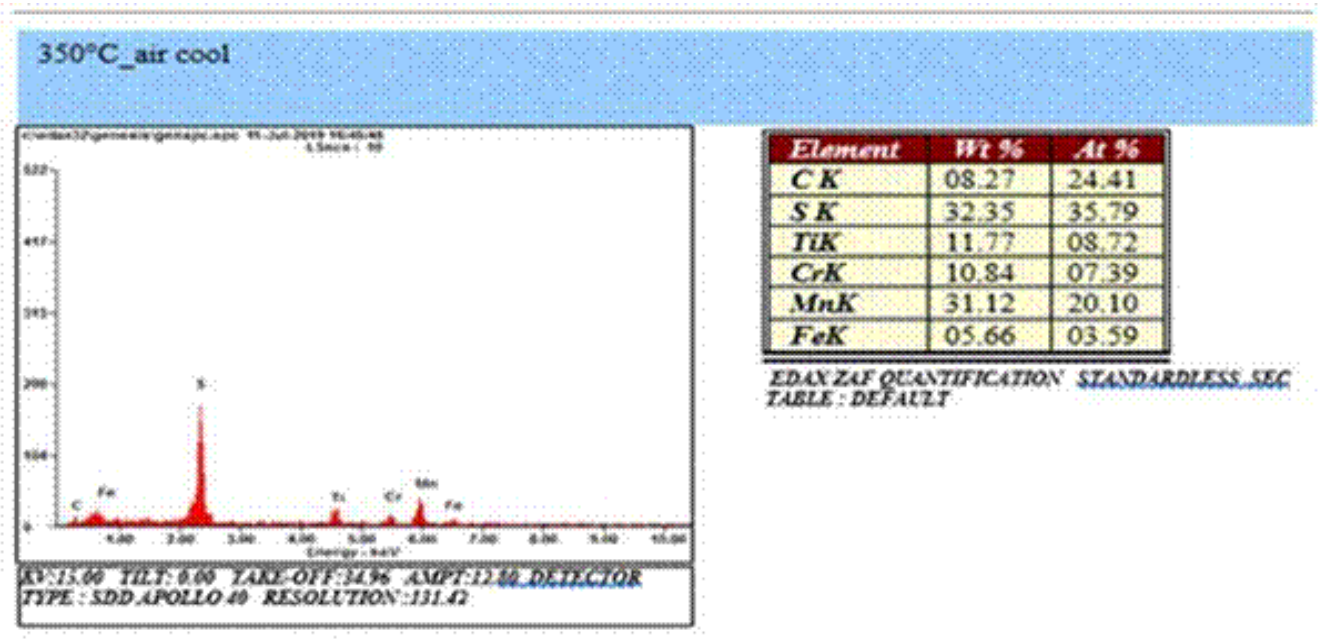

Figure 4.3-EDAX data for martensitic stainless steel heated at350°C for two hours and then air cooled We can see easily that the major inclusion in this sample is MnS which is due to Sulphur already present in the ingot.

4.2.2. Sample heated at 350°C for two hours and then air cooled and then water quenched

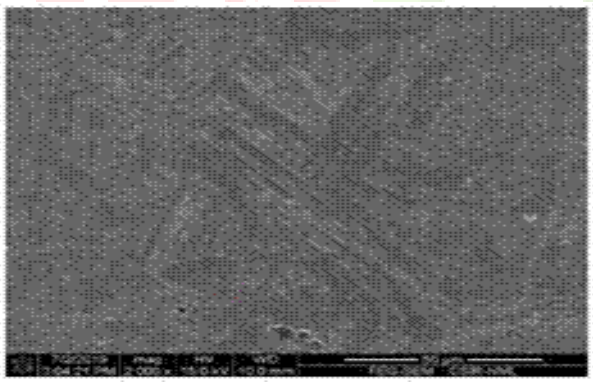

(a)

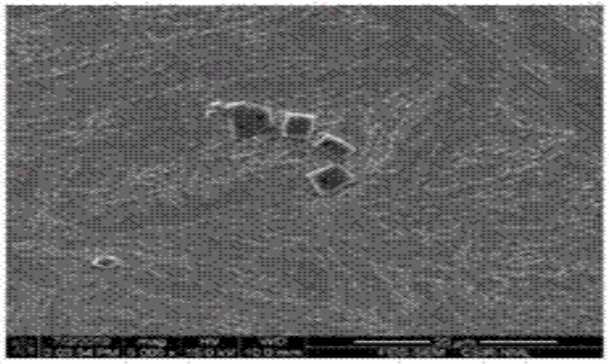

(b)

Figure 4.4-(a) shows the laths of martensite and fig (b) shows the precipitates formed near the grain boundaries and the shape of precipitate is cubical which indicates that it is metal nitrate which is basically (Ti,Al)N.

We can also see that this sample has more martensite than the samples which has been simply air cooled and therefore it will be slightly harder than the above simple air cooled sample. We will see later the hardness relationship between different samples.

4.2.3. Sample heated at 550C for 2 hours and then air cooled

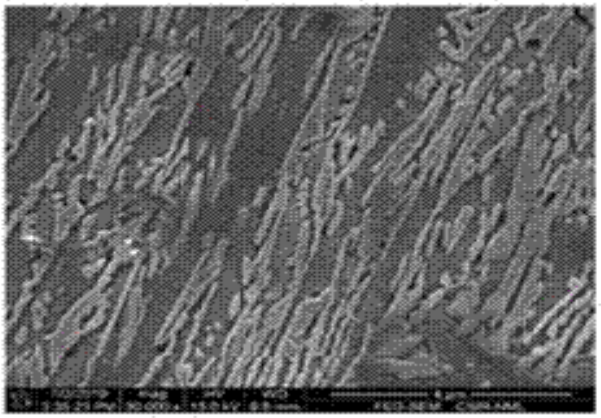

(a)

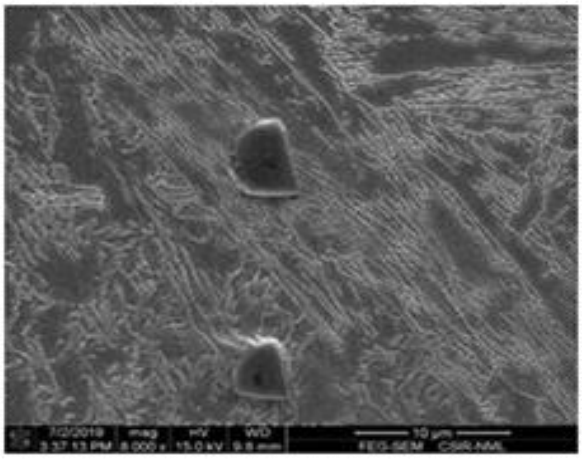

(b)

Figure 4.5-(a) shows the martensite lath (b) shows the microstructure containing (Ti,Al)N.

We can see that this sample has more austenite than the above two samples because due to high temperature treatment the austenite stabilizers has diffuse into the gamma phase and has stabilized the gamma phase.

4.2.4. Samples heated at 550°C for two hours and then air cooled and then aged for 5 hours at 370°C

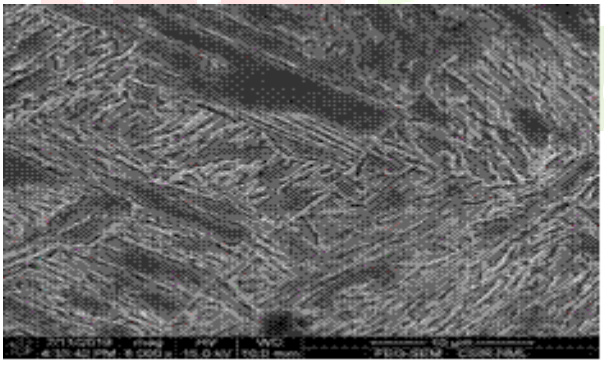

(a)

Figure 4.6-(a) shows the lath martensite present in the aged sample

4.2.5. Sample heat treated at 600°C and then air cooled

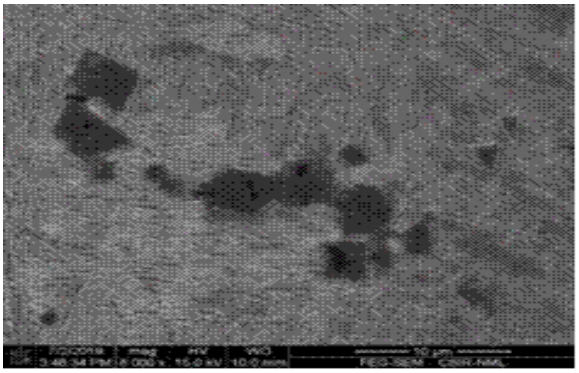

(a)

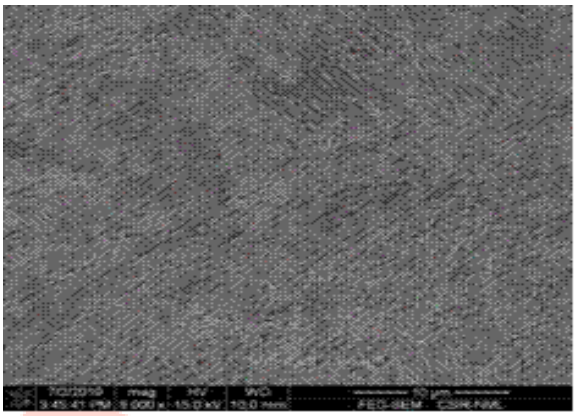

(b)

Figure 4.7-(a) shown the precipitates formed during heat treatment and the precipitate is mainly (Ti,Al)Nand fig(b) shows the dense lath martensite.

4.2.6. Sample heat treated at 600°C for 2 hours and then air cooled and then aged at 370°C for 5 hours

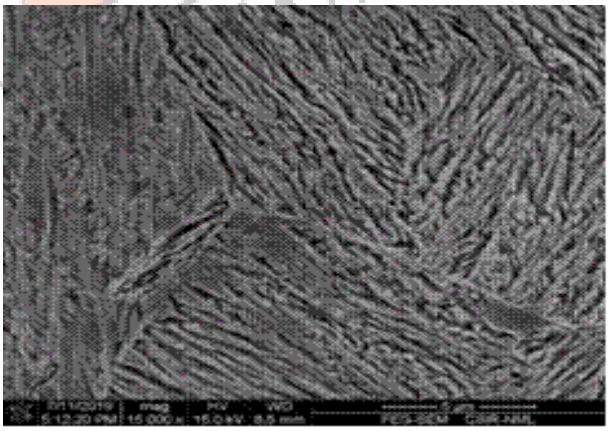

(a)

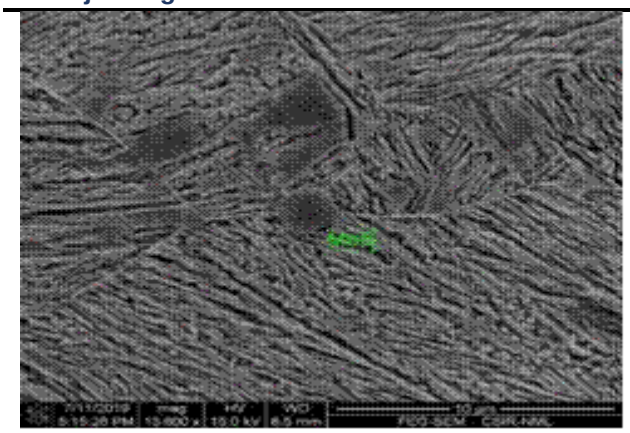

(b)

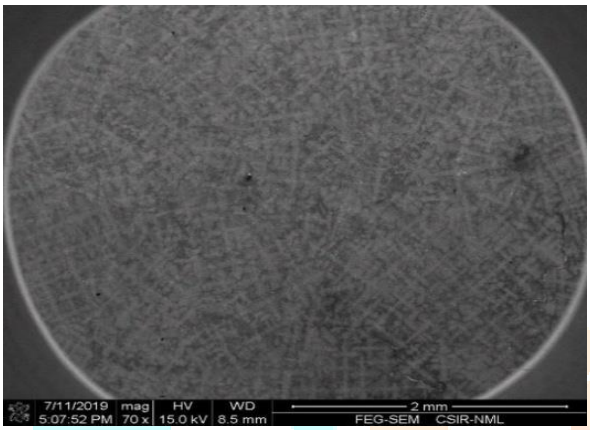

(c)

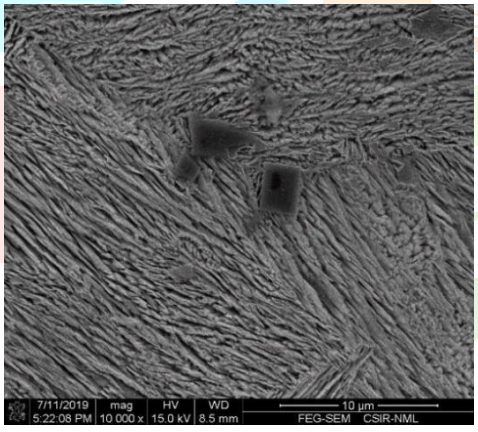

(d)

Figure 4.8-(a) shows very dense lath martensite and fig(b) shows the MnS inclusion which is formed due to the sulphur present in the steel. Fig(c) shows the dendritic like structure which is present in the structure just because that the sample has not undergone any mechanical process like forging, rolling e.t.c. Fig (d) shows the precipitates formed during heat treatment which is mainly (Ti,Al)N which is also shown by EDAX analysis ass shown below:

Figure 4.9-EDAX analysis of sample heat treated at 600°C for 2 hours and then air cooled and then aged at 370°C for 5 hours

We can easily analyse from the curve that the major precipitate formed are Titanium Aluminium

Nitrat

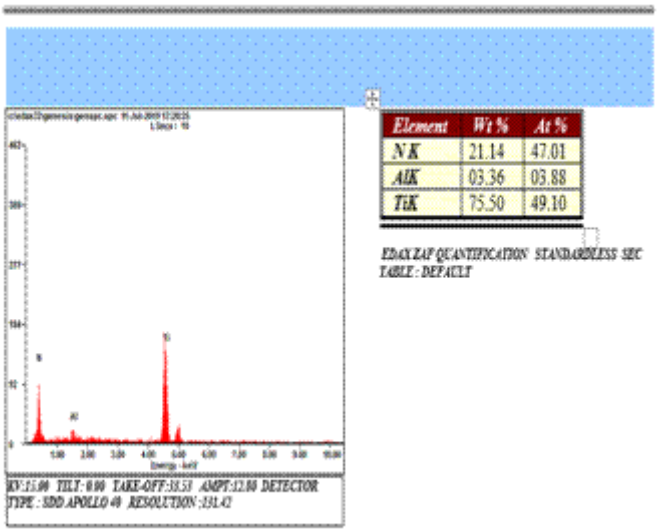

Element	Wt %	At %
N K	21.14	47.01
Al K	03.36	03.88
Ti K	75.50	49.10

EDAX ZAF QUANTIFICATION STANDARDLESS SEC TABLE : DEFAULT

KV:15.00 TILT: 0.00 TAKE-OFF:35.51 AMPT:12.86 DETECTOR TYPE : SDD APOLLO 40 RESOLUTION :131.42

4.2.7. SEM microstructure of as homogenized sample

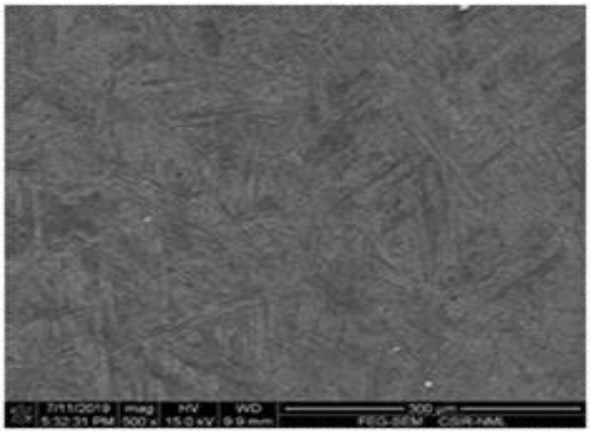

(a)

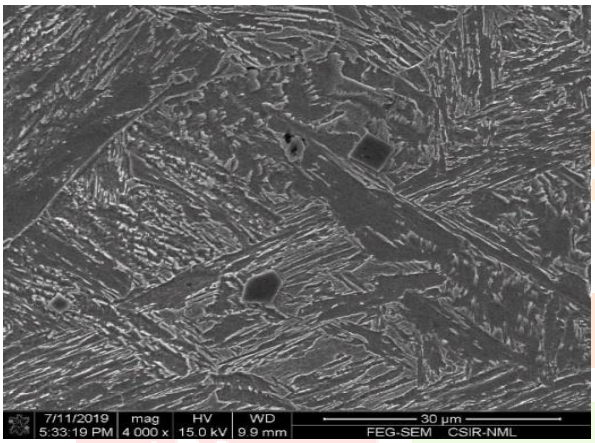

(b)

Figure 4.10-(a) shows the dendritic like structure of the martensitic structure and fig(b) shows the precipitates formed during homogenization which is mainly Titanium Aluminium Nitrate.

4.3. XRD analysis of heat treated samples using integrated intensity

The total integrated intensity of all diffraction peaks for each phase is proportional to the volume fraction of that phase. The phase fraction of retained austenite in specimens obtained by integrated intensity method is given below in table:

Table 4.2. Weight percent of retained austenite after diffe of heat treatment done to martensitic stainless steel of composition.

Heat treatment	Wt.% of retained austenite
Sample heated at 350°C and then air cooled	2.87
Sample heated at 350°C and then air cooled and then quenching in liquid nitrogen	47.34
Sample heated at 550°C and then air cooled	45.18
Sample heated at 550°C and then air cooled and then aged at 370°C for 5 hours	45.61
Samples heated at 600°C and then air cooled	28.52
Samples heated at 600°C and then air cooled and then aged at 370°C for 5 hours	45.22
As homogenized sample	5.24

4.4. Vicker's hardness test of heat treated samples

The hardness of different heat treated material tested at 30 kg load on Vicker hardness machine is shown below in the table

Table 4.3. Vicker's Hardness no. After different kind of heat treatment done to martensitic stainless steel of specific composition.

Sample	Vicker's hardness no.
Sample heated at 350°C and then air cooled	349.67
Sample heated at 350°C and then air cooled and then quenching in liquid nitrogen	350.5
Sample heated at 550°C and then air cooled	306.5
Sample heated at 550°C and then air cooled and then aged at 370°C for 5	332.0
Sample heat treated at 550C and then air cooled and then quenched in	322.5
Samples heated at 600°C and then air cooled	308.67
Samples heated at 600°C and then air cooled and then aged at 370°C for 5	340.33
Samples heated at 600C and then air cooled and then quenched in liquid	317.0
As homogenized sample	333.33

CONCLUSIONS

1. The hardness of the sample heat treated at 350°C then air cooled and then quenched in liquid nitrog highest among the samples.

2. The wt % of retained austenite in samples heat tr at 600°C for 2 hours and then aged at 370°C for 5 ho max.

3. The high hardness sample i.e. sample heat treat 350°C for two hours and then air cooled and the sa heat treated at 350°C for 2 hours and then air coole then quenched in liquid nitrogen has very dense martensite.

REFRENCES

1. Effect of solution treatment temperature on in toughness of a 12Cr-10Ni martensitic precipi hardenable stainless ateel, C. R. Anoop ,Aditya Pra S. V.S. Narayana Murty, Indradev Samajdar.

2. H.Hou.L.Qui.Y.H.Zhao.Effect of austeni temperature on the mechanical properties of strength maraging steel. Material Sci.Engg. A 587 212(2013).

3. D. A. Wigley, Mechanical Properties of Materia low temperature (Plenum Press, New York, 1976)

4. Effect of solution treatment temperature on impact toughness of a 12Cr-10Ni martensitic precipitation hardenable stainless ateel, C. R. Anoop ,Aditya Prakash, S. V.S. Narayana Murty, Indradev Samajdar.

5. H.Hou.L.Qui.Y.H.Zhao.Effect of austenitising temperature on the mechanical properties of high-strength maraging steel. Material Sci.Engg. A 587.209-212(2013).

6. D. A. Wigley, Mechanical Properties of Materials at low temperature (Plenum Press, New York, 1976)

7. 4. U niversidade Federal Fluminense Rua Passo do Patria, 156, CEP 24210-240
   a. Niteroj.RJ.W. B. Lee,S. G. Hong, C. G. Park, K. H. Kim and S. H. Park: Scr. Mater.
   b. 43(2000)319- 324

8. Y. Bai et al.Influence mechanism of parameters process and mechanical properties evolution mechanism of maraging steel 300 by selective laser melting Mater. Sci. Eng. A (2017)

9. Y. Bai et al.Process optimization and mechanical property evolution of AlSiMg0.75 by selective laser melting Mater. Des.(2018)

10. Y. Bai et al.Effect of heat treatment on the microstructure and mechanical properties of maraging steel by selective laser melting Mater. Sci. Eng. A (2019)

11. Y. Bai et al. Investigation on the microstructure and machinability of ASTM A131 steel manufactured by directed energy deposition J. Mater. Process. Technol. (2020)

12. Y. Bai et al. Optical surface generation on additively manufactured AlSiMg0.75 alloys with ultrasonic vibration-assisted machining J. Mater. Process. Technol. (2020)

13. M.J. Bermingham et al. Controlling the microstructure and properties of wire arc additive manufactured Ti-6Al-4V with trace boron additions Acta Mater. (2015)

14. A. Bordin et al. Machinability characteristics of wrought and EBM CoCrMo alloys Procedia CIRP (2014)

15. W. Chen Cutting forces and surface finish when machining medium hardness steel using CBN tools Int. J. Mach. Tools Manuf. (2000)

16. F.F. Conde et al. Effect of thermal cycling and aging stages on the microstructure and bending strength of a selective laser

melted 300-grade maraging steel Mater. Sci. Eng. A(2019)

17. K. Dhale et al. Investigation on chip formation and surface morphology in orthogonal machining of Zr-based bulk metallic glass Manuf. Lett. (2019) View more references Cited by (69)
18. Additive manufacturing of ultra-high strength steels: A review 2023, Journal of Alloys and Compounds Show abstract
19. Machinability of 3D printed metallic materials fabricated by selective laser melting and electron beam melting: A review 2022, Journal of Manufacturing Processes